

Is the Hydrogen Bond in Water Dimer and Ice Covalent?

Tapan K. Ghanty,[‡] Viktor N. Staroverov, Patrick R. Koren, and Ernest R. Davidson*

Contribution from the Department of Chemistry, Indiana University, Bloomington, Indiana 47405

Received October 15, 1999. Revised Manuscript Received December 10, 1999

Abstract: The changes in charge and momentum distributions upon forming a hydrogen bond in the water dimer are examined. The computed Compton profile anisotropies show the same oscillations as were observed for solid ice. These oscillations are already found when the unperturbed orbitals of the water monomers are used to construct a Slater determinant for the dimer. Hence we conclude that the oscillations are irrelevant to the discussion of the covalent character of the bond. Rather they just reflect the result of antisymmetrizing the product of monomer wave functions. In fact, at the oxygen–oxygen distance in ice, the calculations indicate a net antibonding contribution to energy from overlap effects.

Introduction

The hydrogen bonding between water molecules is frequently studied by experimentalists as well as theoreticians.¹ The nearest neighbor O–O distance in ice² is 2.75 Å as compared to 2.98 Å in the gas-phase dimer.³ This change in the O–O distance leads to quite different pictures of the hydrogen bond in the water dimer and ice.^{4–6} One suitable method to understand the nature of the hydrogen bond in a physically meaningful way is to divide the interaction energy into various components such as electrostatic, exchange, dispersion, relaxation, etc. Another approach is to examine changes in other properties such as charge and momentum distributions. Very recently, the anisotropy of the Compton profile for ordinary ice has been interpreted⁷ as direct evidence for partial covalency of the hydrogen bond. The conclusion was based on the fact that the Compton profiles calculated for superimposed water monomers do not exhibit the observed anisotropy, whereas calculations on ice using density-functional theory (DFT) with a pseudopotential and a plane wave basis do predict the observed periodic intensity variations in the Compton profile anisotropies as a function of momentum. This result has been widely publicized in a number of related news articles.^{8–11} There have also been

reports interpreting NMR observations of hydrogen bonds in proteins^{12,13} as a proof of their partial covalency.^{14,15}

In this work our objective is to further explore the H-bond in the water dimer using a recently developed¹⁶ basis set which virtually eliminates the basis set superposition error (BSSE) at the Hartree–Fock level. We have performed a modified Morokuma analysis of the hydrogen bonding in the water dimer at the gas-phase geometry ($R_{OO}=2.98$ Å) as well as in an ice-like dimer ($R_{OO}=2.75$ Å and the angles of the gas-phase dimer) and computed the difference density maps in position and momentum space. For comparison with a system that clearly does not have covalent bonding by most people's definition, we have replaced one water monomer at the ice distance by an isoelectronic Ne atom and performed a similar analysis. We have also computed the Compton profile anisotropies for the water dimer at the O–O distance in ice. The results challenge the above interpretation of the Compton scattering experiment.

Morokuma Analysis of Interaction Energy

The Hartree–Fock portion of the total interaction energy for a dimer (ΔE_{HF}) is defined as the difference between the converged Hartree–Fock energy of the dimer (E_{HF}) and the combined energy of the separated monomers (E_0),

$$\Delta E_{HF} = E_{HF} - E_0 \quad (1)$$

In our modification¹⁷ of the Morokuma method,¹⁸ the interaction energy ΔE_{HF} is partitioned into a sum of electrostatic (ES), exchange (EX), and orbital relaxation (RX) terms. Thus,

$$\Delta E_{HF} = ES + EX + RX \quad (2)$$

Here we have assumed, in agreement with experiment, that the distortion of the geometry of the monomers in the dimer is negligible.

* Address correspondence to this author.

[‡] On leave from the Chemistry Division, Bhabha Atomic Research Centre, Trombay, Bombay 400085, India.

(1) (a) Scheiner, S. *Annu. Rev. Phys. Chem.* **1994**, *45*, 23–56 and references therein. (b) Scheiner, S. *Hydrogen Bonding: A Theoretical Perspective*; Oxford University Press: New York, 1997.

(2) Kuhs, W. F.; Lehmann, M. S. *J. Phys. Chem.* **1983**, *87*, 4312–4313.

(3) (a) Dyke, T. R.; Mack, K. M.; Muentner, J. S. *J. Chem. Phys.* **1977**, *66*, 498–510. (b) Odutola, J. A.; Dyke, T. R. *J. Chem. Phys.* **1980**, *72*, 5062–5070.

(4) Davidson, E. R.; Morokuma, K. *J. Chem. Phys.* **1984**, *81*, 3741–3742.

(5) Yoon, B. J.; Morokuma, K.; Davidson, E. R. *J. Chem. Phys.* **1985**, *83*, 1223–1231.

(6) White, J. C.; Davidson, E. R. *J. Chem. Phys.* **1990**, *93*, 8029–8035.

(7) Isaacs, E. D.; Shukla, A.; Platzman, P. M.; Hamann, D. R.; Barbilini, B.; Tulk, C. A. *Phys. Rev. Lett.* **1999**, *82*, 600–603.

(8) Martin, T. W.; Derewenda, Z. S. *Nat. Struct. Biol.* **1999**, *6*, 403–406.

(9) Helleman, A. *Science* **1999**, *283*, 614–616.

(10) Weiss, P. *Sci. News* **1999**, *155* (No. 4), 52.

(11) Stein, B. P. *Phys. Today* **1999**, *52* (No. 9), 9.

(12) Dingley, A. G.; Grzesiek, S. *J. Am. Chem. Soc.* **1998**, *120*, 8293–8297.

(13) Cordier, F.; Grzesiek, S. *J. Am. Chem. Soc.* **1999**, *121*, 1601–1602.

(14) (a) Cornilescu, G.; Hu, J.-S.; Bax, A. *J. Am. Chem. Soc.* **1999**, *121*, 2949–2950. (b) Cornilescu, G.; Ramirez, B. E.; Frank, M. K.; Clore, G. M.; Gronenborn, A. M.; Bax, A. *J. Am. Chem. Soc.* **1999**, *121*, 6275–6279.

(15) Borman, S. *Chem. Eng. News*, **1999**, *77* (No. 19), 36–38.

(16) Chakravorty, S. J.; Davidson, E. R. *J. Phys. Chem.* **1993**, *97*, 6373–6383.

(17) Frey, R. F.; Davidson, E. R. *J. Chem. Phys.* **1989**, *90*, 5555–5562.

(18) (a) Morokuma, K. *J. Chem. Phys.* **1971**, *55*, 1236–1244. (b) Umeyama, H.; Morokuma, K. *J. Am. Chem. Soc.* **1977**, *99*, 1316–1332.

(c) Morokuma, K. *Acc. Chem. Res.* **1977**, *10*, 294–300.

The ES term is the total Coulombic interaction between the free monomer charge distributions. To evaluate the exchange contribution EX we define an intermediate wave function Ψ_1 , which is the normalized Slater determinant formed from the nonorthogonal molecular orbitals of the free monomers. This Slater determinant is a properly antisymmetrized wave function for the dimer, and is equivalent to one constructed after first orthogonalizing the occupied molecular orbitals of the monomers to each other. The exchange repulsion, EX, due to the repulsive overlap between filled orbitals, is then related to the average energy E_1 of Ψ_1 by

$$EX = E_1 - E_0 - ES \quad (3)$$

The relaxation energy RX is the energy improvement from relaxing the orbitals to their optimum form,

$$RX = E_{\text{HF}} - E_1 \quad (4)$$

In addition, there is a large correlation energy contribution to the binding energy of the water dimer.

This analysis can also be applied to the DFT energy with Slater determinants of Hartree–Fock orbitals replaced by Slater determinants of Kohn–Sham orbitals. In particular, the intermediate system (fully antisymmetrized but unrelaxed) is represented by Ψ_1^{KS} , the Slater determinant formed from the Kohn–Sham orbitals of the monomers. The density corresponding to Ψ_1^{KS} is ρ_1 . The energy E_1 in the definition of the exchange repulsion is the expectation value of the dimer Hamiltonian using Ψ_1^{KS} , i.e., $E_1 = \langle \Psi_1^{\text{KS}} | H | \Psi_1^{\text{KS}} \rangle$, and E_0 is twice the expectation value of the monomer Hamiltonian using the Kohn–Sham orbitals of the free monomer. The subtlety of the DFT energy decomposition is that the EX term then includes not only the exchange $EX_{\text{KS}}^{\text{HF}} = E_1 - E_0 - ES$, but also correlation effects built into the exchange–correlation density functional, i.e.

$$EX = EX_{\text{KS}}^{\text{HF}} + \delta EX_{\text{DFT}} \quad (5)$$

The relaxation energy can be regarded as composed of polarization and charge-transfer components. This partitioning is not clean since it depends on grouping the basis set into functions associated with each monomer. Polarization PL was originally¹⁸ defined as the relaxation energy of one monomer using only its own basis set in the electrostatic field of the other. This definition does not satisfy the Pauli exclusion principle and in the limit of a very extended basis this leads to collapse of the valence electrons of one monomer into the core region of the other. Hence, we have adopted a modified definition¹⁷ according to which the polarization of monomer “A” is computed with all orbitals of A (occupied and virtual) orthogonalized to the Hartree–Fock occupied orbitals of “B” and similarly for the polarization of B. The charge-transfer energy, CT, was computed by allowing orbitals on A that were first orthogonalized to the Hartree–Fock occupied orbitals of B to relax into the virtual orbital space of B. In the limit of a complete basis set on both A and B, the charge transfer and polarization in these definitions become equivalent. In this case, the total relaxation energy of the orbitals of A (orthogonalized to the Hartree–Fock occupied orbitals of B) into the full virtual space, RX-A, would give the same energy as either polarization or charge-transfer alone. Hence, there is significant double counting in these definitions.

In the absence of electron pairing between radicals that characterizes the ordinary Heitler–London covalent bond, it is not clear which part of the total interaction energy should be

Table 1. Morokuma Analysis of Interaction Energies (kcal/mol)

energy components	Hartree–Fock			DFT(B3LYP)
	(H ₂ O) ₂ 2.98 Å	(H ₂ O) ₂ 2.75 Å	Ne·H ₂ O 2.75 Å	(H ₂ O) ₂ 2.75 Å
ES	−7.3	−11.3	−1.4	−11.4
EX	5.5	12.7	5.4	12.5
RX	−1.8	−3.8	−1.0	−5.0
total	−3.6	−2.5	3.1	−3.9
proton donor				
PL	−0.4	−0.8		
CT	−0.3	−0.6		
RX-donor	−0.5	−0.9		
proton acceptor				
PL	−0.6	−1.2		
CT	−1.1	−2.5		
RX-acceptor	−1.3	−2.8		

called “covalent”. Coordinate-covalent bonding (also called donor–acceptor or Lewis acid–base bonding) is usually defined as the sharing of an electron pair of one fragment with an empty orbital of the other. In a minimum basis set description of the water dimer, the highest occupied molecular orbital (HOMO) of the proton acceptor monomer may be thought of as a lone pair orbital on oxygen, while the lowest unoccupied molecular orbital (LUMO) of the donor will be an OH antibonding orbital. The HOMO–LUMO mixing included in the charge-transfer components of the energy could then be regarded as a coordinate-covalent interaction. However, the filled–filled overlap repulsion terms included in EX would not be viewed by most people as an example of “covalency”, since for a system like Ne–Ne it leads to a repulsive Hartree–Fock potential energy curve.

Basis Set and Geometry

The contracted basis sets for oxygen and hydrogen used in this work are the O [7s, 8p, 6d, 1f] and H [4s, 2p, 1d] sets developed earlier by Chakravorty and Davidson.¹⁶ For neon, a similar contracted [8s, 7p, 6d, 1f] basis set has been developed. The *x,y,z* Cartesian coordinates, in bohr, used to perform the calculations for the ice-like dimer ($R_{\text{OO}} = 2.75 \text{ \AA}$), were (0, 0, 0) for the O nucleus of the proton acceptor and (0, 0, 5.196746469) for the O nucleus of the proton donor. The coordinates of the H nuclei were ($\pm 1.430428705, -0.938922356, -0.586703804$), (0, 1.751071514, 5.650256533), and (0, 0, 3.387900752). The gas-phase water dimer differed from this by changing the *z* coordinates of one rigid monomer to the O–O distance of 2.98 Å. With these coordinates, the gas-phase dimer has the experimental geometry of Dyke et al.^{3a} In the Ne·H₂O system, the two hydrogens of the proton acceptor were dropped and the remaining oxygen was replaced by a neon atom. All structures were chosen in such a way that the water monomers have identical geometry. No basis set superposition corrections have been made because the counterpoise correction with this basis set is less than 0.003 kcal/mol in the Hartree–Fock calculation of the dimer.¹⁶

Results

Table 1 summarizes the Morokuma analysis of the Hartree–Fock and DFT (B3LYP) energies for the ice-like water dimer. Also included for comparison are the Hartree–Fock results for the gas-phase dimer. The latter are identical with those published previously.¹⁶ At $R_{\text{OO}} = 2.98 \text{ \AA}$, the electrostatic term is dominant although the exchange repulsion is also large. Relaxation is small but is still half the net Hartree–Fock bonding energy. One could

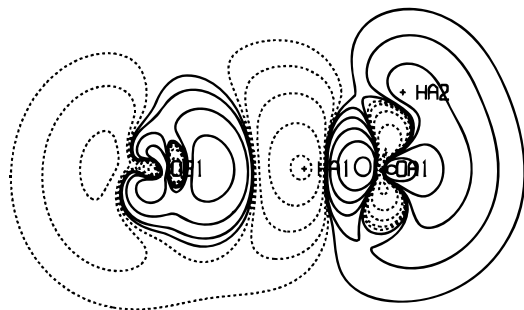


Figure 1. Contour map of the difference between the Hartree-Fock charge density for $(\text{H}_2\text{O})_2$ and the sum of the charge densities for the monomers ($R_{\text{OO}} = 2.75 \text{ \AA}$). The O-O axis is horizontal; the vertical direction is in the mirror plane of the dimer. Solid and dashed lines represent positive and negative differences, respectively. Densities of consecutive levels differ by a factor of $\sqrt{10}$.

claim, perhaps, that the CT contribution to the energy of the proton acceptor (-1.1 kcal/mol) was mostly a HOMO-LUMO mixing and, hence, that part of the interaction would count as coordinate-covalent bonding. As noted above, this view depends critically on a meaningful partitioning of the incomplete basis set between monomers. The additional contribution from electron correlation in the gas-phase dimer is about -1.4 kcal/mol ,¹⁹ so electron correlation (which includes dispersion) is roughly 30% of the total bond energy of -5.0 kcal/mol .¹⁹

At $R_{\text{OO}} = 2.75 \text{ \AA}$, the picture changes substantially even though the total energy is only 1.1 kcal/mol higher. The electrostatic term is more attractive because of the increased penetration of the charge cloud of each monomer into the regions near the nuclei of the other monomer. This same penetration leads to a larger filled-filled overlap and, hence, to a larger exchange repulsion. At this distance, the Slater determinant formed from the MO's of the free monomers actually predicts net repulsion. The relaxation term is correspondingly larger and the CT contribution from the proton acceptor is now accidentally almost equal to the net interaction. Does this mean that the hydrogen bond is "covalent" at the ice distance? There certainly are no new electron pairs being formed, so there is no ordinary Heitler-London covalency. Even though this energy partitioning does point to a nonnegligible HOMO-LUMO mixing, the overlap contributions are dominated by the filled-filled exchange and, hence, are clearly net repulsive.

The B3LYP energy partitioning shows a remarkably similar pattern. The electrostatic interaction computed with DFT is almost the same as the Hartree-Fock value because of the very similar charge distributions for the monomer from Hartree-Fock and DFT. The total exchange repulsion also appears to be largely unaffected by going from Hartree-Fock to DFT. A detailed analysis of the EX value of 12.5 kcal/mol shows that the Fock exchange contribution from the expectation value of the true Hamiltonian with Ψ_1 is $\text{EX}_{\text{KS}}^{\text{HF}} = 14.1 \text{ kcal/mol}$, while the additional contribution of DFT to EX, $\delta\text{EX}_{\text{DFT}}$, is -1.6 kcal/mol . The relaxation term with DFT is even larger than that with Hartree-Fock, so the net attraction is closer to the expected exact value.

The results for the $\text{Ne}\cdot\text{H}_2\text{O}$ system are included in Table 1 to demonstrate that the numbers may be similar even when no one would speak of a covalent bond between the interacting molecules. Because the neon atom is smaller than oxygen, the EX term at $R_{\text{NeO}} = 2.75 \text{ \AA}$ is about the same as that for the

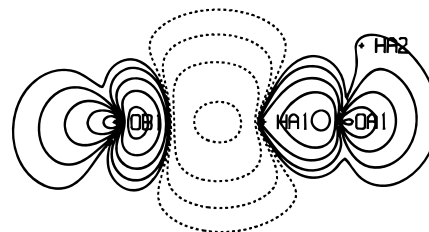


Figure 2. Contour map of the difference between the charge density for Ψ_1 and the sum of the charge densities for the monomers. Conventions as in Figure 1.

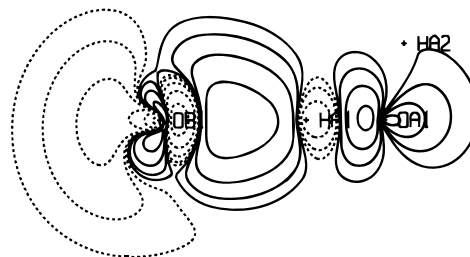


Figure 3. Relaxation of the charge density on the proton acceptor. Conventions as in Figure 1.

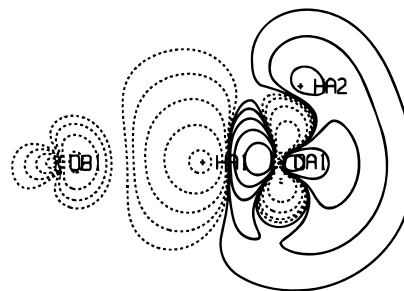


Figure 4. Relaxation of the charge density on the proton donor. Conventions as in Figure 1.

gas-phase water dimer. However, the electrostatic effect is now several times weaker since there are smaller multipole interactions. The relaxation is also smaller because neon is less polarizable. The combination of these three factors leads to a net repulsive interaction.

These results make it clear that there are substantial contributions to the energy from effects that cannot be analyzed by a multipole expansion of the electrostatic and polarization interactions. As we reported in an earlier publication,²⁰ interpenetration of the charge clouds prevents use of the multipole expansion even for the electrostatic part of the energy. The penetration part of the electrostatic energy and the charge transfer and exchange repulsion terms are expected to vary exponentially with the O-O distance.

The total distortion of the charge density in the ice-like water dimer appears in Figure 1. Figure 2 shows the distortion caused by antisymmetry alone, that is, the difference between the density for Ψ_1 and the sum of the densities for the monomers. A substantial depletion of charge in the region between the monomers is observed. Figures 3 and 4 show the total relaxation of charge density on each monomer separately when relaxation into the total virtual space is allowed. Clearly, the largest part of this is polarization, although some charge transfer from the proton acceptor into the OH region of the proton donor is apparent. As we found in an earlier study of the gas-phase dimer,¹⁶ the total charge density distortion is nearly the sum of

(19) Halkier, A.; Klopper, W.; Helgaker, T.; Jørgensen, P.; Taylor, P. R. *J. Chem. Phys.* **1999**, *111*, 9157-9167.

(20) White, J. C.; Davidson, E. R. *J. Mol. Struct. (THEOCHEM)* **1993**, *282*, 19-31.

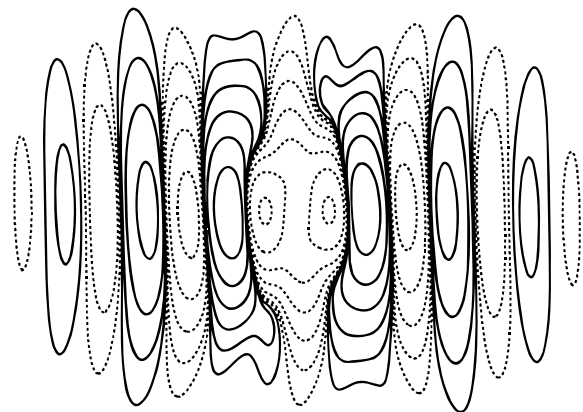


Figure 5. Contour map of the difference between the Hartree-Fock momentum density for $(\text{H}_2\text{O})_2$ and the sum of the momentum densities for the monomers ($R_{\text{OO}} = 2.75 \text{ \AA}$). The direction along the O-O axis is horizontal; the vertical direction is in the mirror plane of the dimer. Zero momentum is in the center of the figure. Densities of consecutive levels differ by a factor of $\sqrt{10}$.

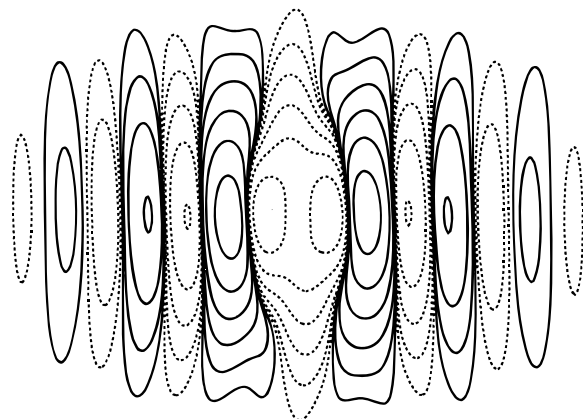


Figure 6. Contour map of the difference between the momentum density for $(\text{H}_2\text{O})_2$ from Ψ_1 and the sum of the momentum densities for the monomers. Conventions as in Figure 5.

the polarization and antisymmetry distortions of each monomer, so the sum of Figures 2, 3, and 4 accounts for most of the effect in Figure 1.

In Figure 5 we show the distortion density in momentum space formed as the difference between the Hartree-Fock momentum density of the ice-like water dimer and the momentum densities of the monomers. These were obtained from the Fourier transforms of the molecular orbitals. The figure has the appearance of a damped plane wave in the direction of the O-O bond with a wavelength of roughly $2\pi/R_{\text{OO}}$. For comparison, Figure 6 shows the distortion caused by antisymmetry alone. It is striking that Figures 5 and 6 are very similar. In contrast, the total relaxation contribution to the momentum density, shown in Figure 7, is much smaller everywhere. Thus, the dominant effect on the momentum density comes simply from antisymmetrizing the product of the free monomer wave functions. The corresponding plots for the gas-phase dimer are essentially identical, as are the plots for the neon-water system. For example, the distortion of the momentum density in the Ne-H₂O system, shown in Figure 8, is very similar to that in Figure 5.

Investigation of bonding effects in liquid water and ion-water clusters by Compton scattering measurements already was a subject of some interest more than 20 years ago.²¹⁻²³ Early theoretical studies of the influence of the hydrogen bonding on the Compton profile of water also date back to that time.^{24,25} The significance of the recent Compton scattering experiment

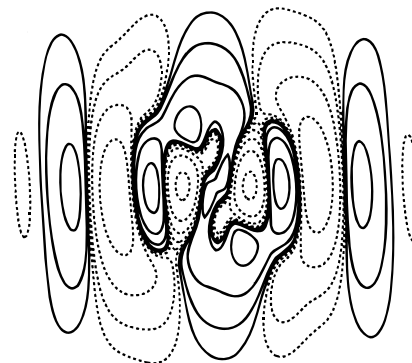


Figure 7. Total relaxation contribution to the momentum density in $(\text{H}_2\text{O})_2$. Conventions as in Figure 5.

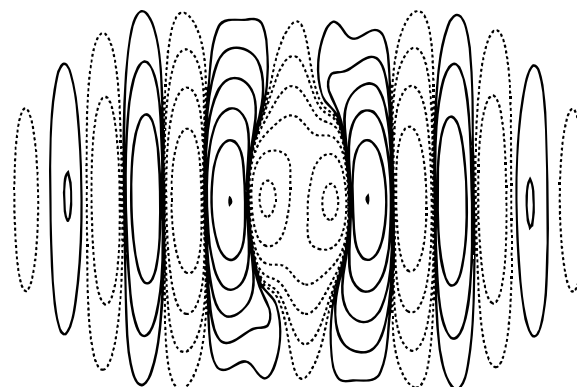


Figure 8. Difference between the Hartree-Fock momentum density for the Ne-H₂O system and the sum of the momentum densities for the isolated Ne atom and H₂O molecule ($R_{\text{NeO}} = 2.75 \text{ \AA}$). The direction along the Ne-O axis is horizontal; the vertical direction is in the mirror plane of the complex. Other conventions as in Figure 5.

on ice by Isaacs et al.⁷ is that it produced for the first time directional rather than spherically averaged Compton profiles for water molecules and allowed a direct comparison of estimated and observed Compton profile anisotropies. For comparison with the discussion by Isaacs et al. of the Compton scattering in ice, we have computed directional Compton profiles for the ice-like water dimer. The directional Compton profile $J(\mathbf{q})$ is defined as the integral of the momentum density over a plane at a distance q from the origin orthogonal to the direction $\hat{\mathbf{q}}$. Figure 9 shows the Compton profile anisotropy, $\delta J(q) = J_{\parallel}(q) - J_{\perp}(q)$, i.e., the difference between the profile along the O-O direction and the profile in the direction orthogonal to the ice-like water dimer mirror plane. The solid and dashed lines, computed with the total momentum densities of the dimer and superimposed monomers, respectively, are nearly identical with the Compton profile anisotropy plots of Isaacs et al.⁷ It is remarkable that the oscillatory structure of the Compton profile anisotropy in real ice is faithfully reproduced with a complex of just two molecules.

Just as the authors of the experiment noted, the plot based on the superimposed monomer density lacks structure while the plot with the actual density shows oscillations. They interpreted

(21) Williams, B. G.; Felsteiner, J.; Halonen, V.; Paakkari, T.; Manninen, S.; Reed, W.; Eisenberger, P.; Weiss, R.; Pattison, P.; Cooper, M. *Acta Crystallogr. Sect. A* **1976**, *32*, 513-526.

(22) Manninen, S.; Paakkari, T.; Halonen, V. *Chem. Phys. Lett.* **1977**, *46*, 62-65.

(23) Paakkari, T. *Chem. Phys. Lett.* **1978**, *55*, 160-162.

(24) Whangbo, M. H.; Smith, V. H., Jr.; Clementi, E.; Dierksen, G. H.; Niessen, v. W. *J. Phys. B: At. Mol. Phys.* **1974**, *7*, L427-L430.

(25) Seth, A.; Baerends, E. J. *Chem. Phys. Lett.* **1977**, *52*, 248-251.

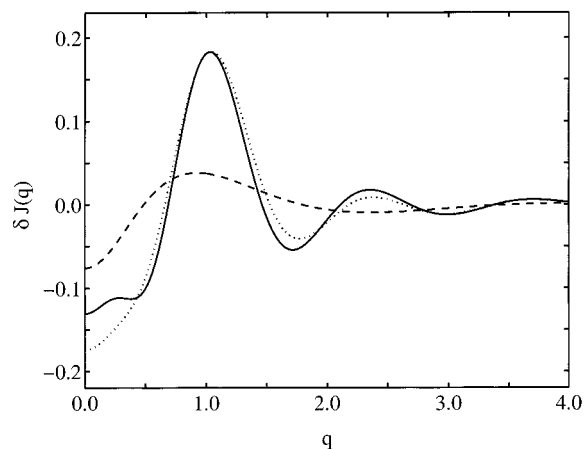


Figure 9. Compton profile anisotropy, $\delta J(q)$, for the ice-like water dimer ($R_{OO} = 2.75 \text{ \AA}$): the difference between the Compton profiles in the O–O direction and in the direction perpendicular to the mirror plane. The solid line is the Hartree–Fock result; the dashed line is for the superposition of the monomers; the dotted line is computed using the antisymmetrized product of the isolated monomer wave functions. Both q and $\delta J(q)$ are in atomic units (\hbar/a_0 and a_0/\hbar , respectively).

these oscillations as a direct experimental proof of the hydrogen bond's partial covalent character. In our figure, however, we have included a third (dotted) curve which is the Compton profile anisotropy computed with Ψ_1 , the unrelaxed Slater determinant of the dimer. In agreement with the observation that Ψ_1 produces nearly the same momentum density as the Hartree–Fock wave function, the directional Compton profiles for Ψ_1 are almost the same as those for the fully relaxed wave function.

Density functional theory is supposed to yield better charge densities than Hartree–Fock. On the other hand, DFT does not produce a meaningful density matrix, so there is no formal justification for using the Fourier transforms of the Kohn–Sham orbitals to construct a momentum distribution. Nevertheless, we have generated similar Compton profile anisotropy plots using Kohn–Sham orbitals in each step. As Figure 10 shows, the DFT curves are nearly indistinguishable from the Hartree–Fock results. As with the Hartree–Fock calculation, the oscillations of the anisotropy plot for the total momentum density are reproduced by the antisymmetrized product of monomer wave functions, but not by the simple product.

Conclusion

The observed difference between the Compton profiles in the O–O direction and the out-of-the-mirror-plane direction in ice are reproduced in the water dimer at the ice O–O distance with either a Hartree–Fock or a Kohn–Sham calculation. This difference is already obtained by merely satisfying the Pauli exclusion principle for the product of the monomer wave functions, but it is not reproduced by adding the monomer densities. Further, the momentum difference maps for the ice-like water dimer, the gas-phase dimer, and the artificial ice-like neon–water system show the same pattern. The difference

(26) King, B. F.; Weinhold, F. *J. Chem. Phys.* **1995**, *103*, 333–347.

(27) Coulson, C. A. *Research* **1957**, *10*, 149–159.

(28) For a qualitative discussion of the directional character of the momentum distribution in chemically bonded systems, see: (a) Epstein, I. R.; Tanner, A. C. In *Compton Scattering*; Williams, B. G., Ed.; McGraw-Hill: New York, 1977; pp 209–233. (b) Tanner, A. C. *Chem. Phys.* **1988**, *123*, 241–247.

(29) Mulliken, R. S. *J. Chem. Phys.* **1955**, *23*, 1833–1840.

(30) Davidson, E. R. *J. Chem. Phys.* **1967**, *46*, 3320–3324.

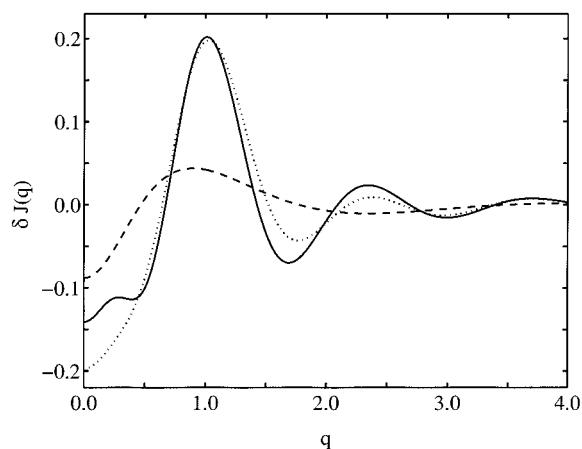


Figure 10. Same as in Figure 9, but using Fourier transformed Kohn–Sham orbitals to generate the momentum density.

densities all have a plane wave appearance that is already present as soon as exchange between monomers is allowed. This plane wave gives rise to the oscillation in the Compton profile anisotropy.

The relaxation charge distributions and Morokuma analysis of the bond energy do show HOMO–LUMO mixing that could be interpreted as a coordinate–covalent interaction. This agrees with the conclusions of Weinhold²⁶ and earlier workers²⁷ and also with our previous calculations.¹⁶ Antisymmetrization of the product of monomer wave functions gives a large exchange repulsion and reduces the charge density between the monomers. This distortion of the orbitals shows up as a filled–filled overlap repulsion and is net antibonding. As we have demonstrated here, the Compton profile measurements are most sensitive to this large antibonding overlap repulsion. Although the news articles imply that the measurements showed a partial covalent attraction, the original paper did note that either bonding or antibonding mixing would lead to oscillations in the Compton profile. However, the authors did not examine the question of whether their calculated wave function showed covalent bonding or antibonding. Certainly they implied that it was bonding by citing earlier theoretical papers concerned with the energy gain from HOMO–LUMO mixing (or, equivalently, from valence bond resonance structures). In fact, calculations of the Compton profile anisotropy, $\delta J(q) = J_{||}(q) - J_{\perp}(q)$, for the simplest molecule H_2^+ show that $\delta J(0)$ is positive for the bonding $1\sigma_g$ state and negative for the antibonding $1\sigma_u^*$ state. The assumption that this principle also holds for many-electron systems and the fact that $\delta J(0)$ is negative for ice suggest that the O...HO interaction is antibonding rather than bonding.²⁸

Another indicator used by chemists for covalent bonding is the Mulliken overlap population.^{29,30} This indicator is basis set dependent and subject to many criticisms. Nevertheless, at both 2.75 and 2.98 \AA the overlap population between the acceptor oxygen and the hydrogen-bonding proton is negative. This again indicates that there is a net antibonding covalent interaction. As expected, the overlap population in the donor O–H bond of the water molecule is less than that in the other three O–H bonds of the dimer. This is consistent with some HOMO–LUMO delocalization into the antibonding O–H orbital of the donor.

Acknowledgment. This work was supported by grant CHE-9613944 from the National Science Foundation.